

The Cytotoxic Enterotoxin of *Aeromonas hydrophila* Induces Proinflammatory Cytokine Production and Activates Arachidonic Acid Metabolism in Macrophages

A. K. CHOPRA,* X.-J. XU, D. RIBARDO, M. GONZALEZ, K. KUHL,
J. W. PETERSON, AND C. W. HOUSTON

Department of Microbiology and Immunology, University of Texas Medical Branch, Galveston, Texas 77555-1070

Received 17 December 1999/Returned for modification 18 January 2000/Accepted 17 February 2000

An aerolysin-related cytotoxic enterotoxin (Act) of *Aeromonas hydrophila* possesses multiple biological activities, which include its ability to lyse red blood cells, destroy tissue culture cell lines, evoke a fluid secretory response in ligated intestinal loop models, and induce lethality in mice. The role of Act in the virulence of the organism has been demonstrated. In this study, we evaluated the potential of Act to induce production of proinflammatory cytokines associated with Act-induced tissue injury and Act's capacity to activate in macrophages arachidonic acid (AA) metabolism that leads to production of eicosanoids (e.g., prostaglandin E₂ [PGE₂]). Our data indicated that Act stimulated the production of tumor necrosis factor alpha and upregulated the expression of genes encoding interleukin-1 β (IL-1 β) and IL-6 in the murine macrophage cell line RAW264.7. Act also activated transcription of the gene encoding inducible nitric oxide synthase. Act evoked the production of PGE₂ coupled to the cyclooxygenase-2 (COX-2) pathway. AA is a substrate for PGE₂, and Act produced AA from phospholipids by inducing group V secretory phospholipase A₂. We also demonstrated that Act increased cyclic AMP (cAMP) production in macrophages. cAMP, along with PGE₂, could potentiate fluid secretion in animal models because of infiltration and activation of macrophages resulting from Act-induced tissue injury. After Act treatment of RAW cells, we detected an increased translocation of NF- κ B and cAMP-responsive element binding protein (CREB) to the nucleus using gel shift assays. Act also upregulated production of antiapoptotic protein Bcl-2 in macrophages, suggesting a protective role for Bcl-2 against cell death induced by proinflammatory cytokines. The increased expression of genes encoding the proinflammatory cytokines, COX-2, and Bcl-2 appeared correlated with the activation of NF- κ B and CREB. This is the first report of the detailed mechanisms of action of Act from *A. hydrophila*.

Aeromonas spp. recently have been placed in the family *Aeromonadaceae*. They cause both intestinal and nonintestinal infections in humans (12), and, unlike gastroenteritis, which generally occurs in young children, these nonintestinal infections are often fatal and involve adults (36). *Aeromonas* spp. have been cultured from both freshwater and salt water and from many foods. These bacteria have emerged as important human pathogens and are being isolated in an increased incidence from patients with traveler's diarrhea (3, 11, 28, 29, 41, 44, 70). *Aeromonas* spp. produce an array of virulence factors, and the pathogenesis of *Aeromonas* infections is therefore complex and multifactorial (2). These virulence factors include hemolysins, cytotoxins, enterotoxins, proteases, lipases/phospholipases, leucocidin, endotoxin, fimbriae or adhesins, and the capacity to form an S-layer (17, 45, 47). *Aeromonas hydrophila* has been shown to be invasive for HEp-2 cell monolayers, and the bacterial cells adhere to human erythrocytes (6, 26). Two distinct families of type IV pili (bundle-forming pili [Bfp] and Tap) in *Aeromonas* spp. are associated with gastroenteritis (9). Taken together, the ability of these bacteria to invade host cells and disseminate to virtually any organ via the blood and their capacity to produce multiple virulence factors contribute to the pathogenesis of *Aeromonas* infection. The ability of some strains of *A. hydrophila* to resist complement-mediated lysis could result in bacteremia and other invasive diseases associated with *Aeromonas* infections (46, 48).

Both cytotoxic and cytotoxic enterotoxins have been discovered in culture filtrates of *Aeromonas* isolates (5, 13, 15, 32, 43, 55, 56, 58, 66). We demonstrated that these enterotoxins from diarrheal isolate SSU of *A. hydrophila* were able to cause intestinal fluid loss in a rat/rabbit model (20, 58, 69). The cytotoxic enterotoxin (Act) is a single-chain, 52-kDa polypeptide that has various biological activities, including hemolysis, cytotoxicity, enterotoxicity, and lethality (18, 23). The cytotoxic enterotoxin gene (*act*) has been hyperexpressed, and the recombinant Act has been purified to homogeneity. The 50% lethal dose of Act for mice was 27.5 ng (23). Act exhibited significant homology with aerolysin isolated from *Aeromonas bestiarum* (originally classified as *A. hydrophila*) (18, 33, 35); however, these molecules were distinguishable from each other by the following criteria: (i) differential neutralization of Act using Act- and aerolysin-specific monoclonal antibodies (19; unpublished data); (ii) different essential amino acid residues in Act and aerolysin which contribute to hemolytic activity (24); and (iii) inability of Act to bind to glycophorin, the aerolysin receptor (25). We have shown that cholesterol, but not myristylated cholesterol, abrogated Act's hemolytic activity, and this finding implicated the 3'-OH group of cholesterol as possibly important for toxin interaction with this membrane constituent (23). Despite these distinguishing features, Act and aerolysin have both been shown to be activated by binding to the target cell membrane, with subsequent oligomerization and pore formation (16, 23, 50).

Most studies on aerolysin were targeted to measuring hemolytic activity (50); however, site-directed mutagenesis of a single chain of Act indicated the possibility of different loci

* Corresponding author. Mailing address: Department of Microbiology and Immunology, UTMB, Galveston, TX 77555-1070. Phone: (409) 747-0578. Fax: (409) 747-6869. E-mail: achopra@utmb.edu.

associated with various biological activities (24). We identified an Act peptide (amino acid residues 245 to 274) that competed with native Act in binding to Chinese hamster ovary (CHO) cells. Further, polyclonal antibodies to this peptide significantly neutralized Act's biological activity (24). Act's role in the overall virulence of the organism has been established by developing transposon mutants of *A. hydrophila* SSU and by generating *act* isogenic mutants via homologous recombination (69). When isogenic mutants were injected intraperitoneally into mice, the 50% lethal dose was found to be 10^8 compared to 3×10^5 for the wild-type *Aeromonas*. Reintegration of the native *act* gene in place of the truncated toxin gene in isogenic mutants resulted in complete restoration of Act's biological activity and virulence in mice. Animals that were injected with a sublethal dose of wild-type *Aeromonas* or its revertant, but not the isogenic mutant, had circulating, toxin-specific neutralizing antibodies (14, 69). Act-induced fluid secretion in the rat and rabbit ligated small intestinal loop was accompanied by inflammation with infiltration of mononuclear cells in the lumen of the intestine. However, whether there is a correlation between the extent of inflammation induced by Act and fluid secretion at various toxin doses is unknown and is presently under investigation. Act impaired the phagocytic ability of mouse phagocytes, both in vivo and in vitro, and gamma interferon (IFN- γ) pretreatment blocked this toxic effect. Act's direct inhibition of phagocyte activity may be a pathological mechanism associated with some *Aeromonas*-mediated infections (38). Further, Act significantly stimulated the chemotactic activity of human leukocytes in a dose-dependent fashion. This stimulatory effect was inhibited by various concentrations of pertussis toxin (PT), suggesting that human leukocytes possessed Act receptors possibly coupled to PT-sensitive G-proteins (37). Recent studies of Krause et al. (42) showed that aerolysin, like Act, activated PT-sensitive G-proteins in granulocytes.

In this study, we examined the mechanism of action of Act by using murine macrophages to determine whether Act up-regulated the expression of proinflammatory cytokine genes and the inducible nitric oxide synthase (iNOS) gene and activated arachidonic acid (AA) metabolism in these cells. The latter mechanism results in production of eicosanoids (e.g., prostaglandin E_2 [PGE_2]) that activate adenylate cyclase and produce cyclic AMP (cAMP). The latter can also be produced through direct activation of a G-protein-coupled adenylate cyclase enzyme in cells. The fluid secretory response observed in animals with Act therefore could be a result of an Act-induced inflammatory response and the ability of Act to increase PGE_2 and cAMP levels. Finally, we identified transcription factors activated in Act-treated macrophages to understand intracellular signaling in host cells leading to upregulation of genes encoding various cytokines, cyclooxygenase-2 (COX-2), and antiapoptotic protein Bcl-2.

MATERIALS AND METHODS

Cell culture. The murine macrophage cell line RAW264.7 was purchased from the American Type Culture Collection (Manassas, Va.). The cells were cultured at 37°C and 5% CO_2 in Dulbecco's minimal essential medium (Gibco BRL, Gaithersburg, Md.) containing 4.5 g of glucose/liter, 10% fetal bovine serum, 2 mM L-glutamine, and antibiotics penicillin (100 U/ml) and streptomycin (0.1 mg/ml). For each experiment, 5×10^5 cells/ml were plated in 35-mm-diameter dishes and allowed to attach for 60 min. The medium was removed, and fresh medium containing the appropriate stimulant was added. After each time point, the supernatant was collected and Trizol reagent (Gibco BRL) was added to the cells (1 ml per 10^6 cells) to extract RNA and proteins as described by the manufacturer.

Northern analysis. Total RNA (10 to 20 μ g) was separated in a 3% formaldehyde gel (7) and transferred to a nylon membrane. Membranes were prehybridized (15 min) and hybridized using Quickhyb (Stratagene, La Jolla, Calif.).

The radioactive counts for the various probes used were all 10^6 cpm/ml, and the probes were applied to membranes in Quickhyb solution for 2 h at 68°C. After incubation, membranes were washed twice for 20 min in $2 \times$ SSC ($1 \times$ SSC is 0.15 M sodium chloride plus 0.015 M sodium citrate), pH 7.0 (7)–0.1% sodium dodecyl sulfate (SDS) and twice for 20 min in $1 \times$ SSC–0.1% SDS at 68°C. When group V secretory phospholipase A_2 (sPLA $_2$) was used as a probe, membranes were hybridized for 1 h at 66°C, followed by two washes in $2 \times$ SSC–0.05% SDS for 15 min, with the first wash at room temperature and the second at 40°C. Membranes were then washed twice with $0.1 \times$ SSC–0.1% SDS for 15 min at room temperature (8), dried, and exposed to X-ray film for 1 to 3 days. The membranes were subsequently stripped in $2 \times$ SSC–50% formamide at 68°C for 2 h and rehybridized with a glyceraldehyde-3-phosphate dehydrogenase (GAPDH) (Clontech Laboratories Inc., Palo Alto, Calif.) probe as an internal control. The RNA load in each lane was normalized by densitometric scanning (Gel doc 2000 system; Bio-Rad, Hercules, Calif.) of the blots to calculate fold increases in mRNA levels. The probes were labeled with [α - 32 P]dCTP (ICN; Costa Mesa, Calif.) using a random priming kit (Gibco BRL) and the unincorporated dCTP was removed using a Sephadex G-25 spin column (5'–3' Inc., Boulder, Colo.). Murine tumor necrosis factor alpha (TNF- α) cDNA was generated by reverse transcriptase PCR (RT-PCR) as described below using specific TNF- α RT-PCR amplimers (Clontech) and total RNA from RAW cells. A 354-bp cDNA was cloned into TA cloning vector pCR2.1 (Invitrogen, Carlsbad, Calif.). The recombinant plasmid was digested with the *Eco*RI restriction enzyme to obtain a 354-bp cDNA fragment. Murine interleukin-1 β (IL-1 β) cDNA (Genentech, Inc., San Francisco, Calif.) was digested with *Eco*RI and *Hind*III restriction enzymes, and a 1.3-kb fragment generated was used as a probe. The DNA fragments were isolated from 0.8% agarose gels (7) and purified using GeneClean kit II (Bio 101, Inc., Vista, Calif.). A *cox-2* cDNA probe used for Northern analysis was purchased from Cayman Biochemical Co., Ann Arbor, Mich.). The reagents for RNA work were prepared in diethyl pyrocarbonate (DEPC)-treated water.

Western blot analysis. Western blot analysis was performed by established procedures (59). Briefly, equal amounts of total protein were loaded and separated on SDS–12% polyacrylamide gels and then transferred to nitrocellulose membranes. Membranes were blocked with 3% gelatin and washed in $1 \times$ Tween (0.05%)–Tris-buffered saline (TTBS) twice for 10 min each. Primary antibodies (1 to 15 μ g/ml) in a 1% gelatin solution (prepared in $1 \times$ TTBS) were applied and allowed to incubate for 2 h at room temperature. After washing, appropriate secondary antibodies were diluted 1:30,000 for horseradish peroxidase (HRP) or 1:10,000 for alkaline phosphatase (AP) in 1% gelatin and applied to the membranes. Subsequently, membranes were washed and an appropriate substrate was applied, according to the manufacturer's instructions for color development, using AP substrate (Bio-Rad) or an enhanced chemiluminescence substrate kit (Pierce, Rockford, Ill.). Polyclonal COX-2, inducible nitric oxide synthase (iNOS), and Bcl-2 antibodies were purchased from Santa Cruz Biochemical Co., Santa Cruz, Calif.

RT-PCR to detect various cytokines. The first-strand cDNA synthesis kit (Clontech) was used to synthesize cDNA from total RNA of RAW cells as described by the manufacturer. Briefly, to 1 μ g of total RNA was added oligo(dT) $_{18}$ primer (20 μ M) in a total volume of 12.5 μ l made up with DEPC-treated water. The RNA and primer were heated at 70°C for 2 min and then quenched on ice immediately. Subsequently, the following reagents were added: 4.0 μ l of 5 \times reaction buffer (Clontech), 1.0 μ l of deoxynucleoside triphosphate (dNTP) mixture (10 mM each), 0.5 μ l of recombinant RNase inhibitor (40 U/ μ l), and 1.0 μ l of recombinant Moloney murine leukemia virus RT (200 U/ μ l). The mixture was incubated at 42°C for 1 h, and the cDNA synthesis was stopped by heating the reaction mixture at 94°C for 5 min, which also destroyed any remaining DNase activity. The reaction mixture was then diluted to a final volume of 100 μ l with DEPC-treated water.

The cDNA fragment was amplified by PCR, and the following reagents were added to 5 μ l of cDNA sample: 5 μ l of $10 \times$ PCR buffer (Promega, Madison, Wis.), 36.6 μ l of sterile water, 1 μ l of dNTP mixture (10 mM each), 0.4 μ l of AmpliTaq DNA polymerase (5 U/ μ l), 2 μ l of premixed human GAPDH amplimer (10 μ M [each] primer; for internal control), and 1 μ l each of the tested 5' and 3' primers (20 μ M) for mouse IL-1 β (fragment size, 563 bp) and mouse IL-6 (fragment size, 638 bp). The amplimers were obtained from Clontech. The PCR was then completed by temperature cycling (30 to 35 cycles of 94°C for 45 s, 60°C for 45 s, and 72°C for 2 min and a final extension at 72°C for 7 min). The PCR product was run on a 1% agarose gel and subjected to densitometric scanning, and the fold increase in the level of a particular cytokine cDNA was normalized to the GAPDH product. Each experiment included a negative control in which RNA was omitted from the RT mixture and cDNA was omitted from the PCR.

The group V sPLA $_2$ fragment for Northern blot analysis was generated by first performing reverse transcription using RNA from RAW cells, as described above, followed by PCR using the following primers: 5'CAGGGGGCTTGCTA GAACCTCAA3' (5' primer) and 5'AAGAGGGTGTGAAGTCCAGAGG3' (3' primer) as described by Balboa et al. (8). A sample probe was obtained from E. A. Dennis, University of California at San Diego, La Jolla. Reaction conditions used for PCR were 95°C for 20 s, 60°C for 30 s, and 72°C for 30 s for 35 cycles, followed by a final extension at 72°C for 7 min.

ELISA. The purified anticytokine capture antibodies (Pharmingen, San Diego, Calif.) were diluted to 1 to 4 $\mu\text{g/ml}$ in binding solution (0.1 M Na_2HPO_4 , pH 9.0). The diluted antibodies then were added to the wells of an enzyme immunoassay high-binding microtiter plate (Corning Costar, Corning, N.Y.) and incubated overnight at 4°C. Next, the capture antibodies were removed, and any nonspecific binding was blocked by adding 200 μl of blocking buffer (1% bovine serum albumin in phosphate buffered saline [PBS]) to each well. The plate was incubated at room temperature for 1 to 2 h. After incubation, wells were washed three times with PBS-Tween (0.05%) buffer. A 100- μl aliquot of samples or standards was added, and the plate was incubated overnight at 4°C. After incubation, plates were washed four times with PBS-Tween. Detection antibodies (biotinylated anticytokine; Pharmingen) were diluted to 0.5 to 2 $\mu\text{g/ml}$ in blocking buffer-Tween and added to the wells. The plate was incubated for 1 h at room temperature. After the plate was washed four times with PBS-Tween, an enzyme conjugate (streptavidin-conjugated HRP) was diluted to an optimal concentration in blocking buffer-Tween and added to the wells. The plate was incubated at room temperature for 30 min and then washed five times with PBS-Tween. Next, ABTS [2,2'-azino-bis-(3-ethylbenzthiazoline-6-sulfonic acid)] substrate solution (150 mg of ABTS in 0.1 M anhydrous citric acid, adjusted to pH 4.35 with sodium hydroxide) was vortexed, and 100 μl of 3% H_2O_2 was added to each 11 ml of substrate solution. A 100- μl aliquot was dispensed in each well, and the plate was incubated (5 to 80 min) for color development. The color reaction was stopped by adding 50 μl of stopping solution (20% SDS–50% dimethyl formamide). Finally, the optical density was read with a microtiter enzyme-linked immunosorbent assay (ELISA) plate reader (Molecular Devices Corp., Sunnyvale, Calif.) at 405 nm.

Gel shift assay. Labeling of the consensus oligonucleotide was performed by assembling the following reaction mixture: 2 μl of NF- κB /CREB/AP-1/AP-2/SP-1 (promoter-specific factor required for transcription of the simian virus 40 early and late promoters)/OCT-1 (octamer transcription factors)/TFIID (general transcription factors) consensus oligonucleotide (1.75 pmol/ μl ; Promega), 1 μl of T4 polynucleotide kinase 10 \times buffer (Promega), 1 μl of [γ - ^{32}P]ATP (3,000 Ci/mmol at 10 mCi/ml; ICN), 5 μl of nuclease-free water, and 1 μl of T4 polynucleotide kinase (5 to 10 U/ μl ; Promega). The reaction mixture was incubated at 37°C for 10 min, and the reaction was stopped by adding 1 μl of 0.5 M EDTA. Finally, the volume of the reaction mixture was made up to 100 μl using 1 \times Tris-EDTA buffer (7) before the mixture was passed through the Sephadex G-25 spin column to remove unincorporated labeled ATP. Next, DNA binding reaction mixtures were assembled. For this assay, we utilized a negative control having no HeLa cell nuclear extract and a positive control consisting of HeLa cell nuclear extract, a specific competitor such as unlabeled transcription factor consensus oligonucleotides, and nuclear extracts from specific time points after Act treatment of RAW cells. The nuclear extracts were prepared as described by the manufacturer (Promega). The reaction mixtures were incubated at room temperature for 5 to 10 min. Then, 50,000 to 200,000 cpm of ^{32}P -labeled transcription factor consensus oligonucleotide was added to the reaction mixtures, and the mixtures were incubated at room temperature for 20 min. For supershift assays, 2 μl of p50, p65, or CREB antibodies (200 $\mu\text{g}/0.1$ ml; Santa Cruz Biotechnology) was added to the reaction mixture prior to the addition of labeled NF- κB and CREB consensus oligonucleotides. Subsequently, 1 μl of gel loading 10 \times buffer (Promega) was added to each reaction mixture and samples (5 to 10 μg) were loaded on a nondenaturing 4% polyacrylamide gel. The gel was prerun in 0.5 \times Tris-borate-EDTA buffer for 30 min at 70 mA before loading the samples. After completion of the run, the gel was transferred to Whatman 3 MM paper, dried at 80°C for 2 h, and exposed to X-ray film for 1 h to overnight with an intensifying screen.

cAMP measurement. cAMP was measured by manufacturer's protocols (PerSeptive Biosystems, Framingham, Mass.). Briefly, 100 μl of sample, standard, or medium alone, in duplicate, was pipetted into a 96-well plate precoated with goat anti-rabbit antibody. A 100- μl aliquot of cAMP antibody was applied and allowed to incubate for 2 h at 4°C. After this incubation, 100 μl of cAMP conjugated to AP was added to the wells and allowed to incubate for 1 h at 4°C. After incubation, wells were washed six times with wash buffer (Tris-buffered saline–0.01% thimerosal) and an aliquot (300 μl) of para-nitrophenyl phosphate substrate solution was added to each of the wells. After incubation for 2 h at 37°C, the reaction was stopped by the addition of 50 μl of stop solution (0.2 N NaOH) to each of the wells, followed by absorbance readings taken at 405 nm.

PGE₂ assay. PGE₂ was measured by the manufacturer's protocol (Amersham Pharmacia). Briefly, 50 μl of sample, standard, or medium alone, in duplicate, was pipetted into a 96-well plate precoated with goat anti-mouse antibody. A 50- μl aliquot of PGE₂ antibody and 50 μl of PGE₂ conjugated to AP were added to the wells and allowed to incubate for 1 h at room temperature. After incubation, wells were washed six times with wash buffer (0.01 M PBS–0.05% Tween) and a 150- μl aliquot of 3,3',5,5'-tetramethylbenzidine–hydrogen peroxide (in 20% dimethyl formamide) substrate solution was applied to each of the wells. After incubation for 30 min at room temperature, the plate was read at 650 nm in an ELISA reader.

PLA₂ assay. [^3H]AA-labeled *Escherichia coli* (DuPont NEN Research Products, Boston, Mass.) was used as the substrate for measuring PLA₂ activity (61, 62). Briefly, the reaction mixture consisted of the following: 10 μl of 2-mg/ml bee venom PLA₂ (Sigma, St. Louis, Mo.; positive control), water (negative control), or culture supernatant of RAW cells treated with Act for various periods of time;

20 μl of water; 10 μl of assay buffer (500 mM Tris-HCl [pH 8.0], 500 mM NaCl, 5 mg of bovine serum albumin/ml, 50% glycerol, 1 mM CaCl_2); and 10 μl of [^3H]labeled *E. coli* cells. The samples were mixed and incubated at 37°C for 15 min. Subsequently, the reaction was stopped by adding three times the volume (150 μl) of cold PBS. The samples were vortexed and centrifuged at 10,000 $\times g$ for 10 min at 4°C, and an aliquot of the supernatant (50 μl) was mixed with 4 ml of scintillation fluid and counted using a β -counter.

Purification of Act. For these studies, we expressed the *act* gene from broad-host-range *tac* promoter-based vector pMMB66 (American Type Culture Collection) in *Aeromonas salmonicida*. The *act* gene was induced with 1 mM isopropyl- β -D-thiogalactopyranoside (IPTG) (23). The coding region of the *act* gene was cloned into a pMMB66EH vector at the *EcoRI* and *HindIII* sites using the following 5' and 3' primers: 5'CGGAATTCATGCAAAACTAAAAATACTGGCTTG3' and 5'ATAAGCTTTATTGATTGGCTGCTGGCGTCACGCT3'. The underlined bases represent 5' *EcoRI* and 3' *HindIII* sites. The recombinant plasmid first was transformed into *E. coli* HB101 carrying helper plasmid pRK2013, which conferred kanamycin resistance. Subsequently, the recombinant pMMB66 plasmid was transformed into a spontaneous rifampin-resistant mutant of *A. salmonicida* via conjugation (69). This *Aeromonas* strain did not harbor the gene for Act, and the rifampin resistance marker allowed differentiation of *Aeromonas* from *E. coli* after conjugation. The transconjugants were screened on Luria-Bertani (LB) agar plates containing rifampin (40 $\mu\text{g/ml}$), kanamycin (25 $\mu\text{g/ml}$), and ampicillin (100 $\mu\text{g/ml}$). *A. salmonicida* (pMMB66act) was grown in LB medium with appropriate antibiotics at 26°C. At an optical density of 0.4, the culture was induced with 1 mM IPTG for 2 h. The culture filtrate was subjected to ammonium sulfate precipitation (60% saturation), followed by sequential chromatography on a Resource Q column (Amersham Pharmacia), a phenyl-Sepharose column, and a hydroxyapatite column (Bio-Rad) using Akta Purifier 10 (Amersham Pharmacia) (23). Approximately 1 mg of the pure toxin was obtained from 2 liters of the culture with 40% total recovery. Silver staining and NH₂-terminal amino acid sequence analysis confirmed the purity of Act.

LPS contamination of Act preparation. The *Limulus* amoebocyte lysate assay (OCL-1000 kit; BioWhittaker, Walkersville, Md.) was used to determine the level of lipopolysaccharide (LPS) contamination in the purified Act. In addition, the effect of polymyxin B sulfate (which inactivates LPS) on Act's ability to induce production of various cytokines also was determined. Purified Act was incubated with polymyxin B sulfate (Sigma) at a concentration of 10 $\mu\text{g/ml}$ for 30 min on ice before use. This concentration of polymyxin was sufficient to abrogate up-regulation of proinflammatory cytokine genes by LPS (20 ng/ml) in RAW cells.

Statistical analysis. The data were analyzed by a multiple group comparison test (Scheffe), which allowed all groups to be compared with each other, and hence is the most stringent statistical method available.

RESULTS

Act induced production of proinflammatory cytokines in macrophages. When murine macrophages (RAW264.7) were treated with purified Act, the abundance of TNF- α mRNA increased within 30 min, based on Northern analysis. An approximately 200-fold increase in the TNF- α mRNA level was noted when macrophages were treated with Act for 2 h and was followed by a decline in the TNF- α mRNA levels that remained constant between 4 and 24 h (Fig. 1A). The concentration of Act selected for these experiments was 6 ng/ml, which did not kill macrophages. After 24 h of toxin treatment, the cell viability was 98 to 99% as measured by trypan blue exclusion. An increase in the TNF- α antigen level also was detected at 30 min, and the level gradually increased for up to 24 h (14,000 pg/ml) based on an ELISA (Fig. 1B). Likewise, an increase in the IL-1 β mRNA level was apparent within 30 min to 2 h of Act exposure to the cells; however, a maximum increase (130-fold) in the abundance of the IL-1 β mRNA was noted after 4 h of Act treatment (Fig. 2). A dramatic reduction in the mRNA level of IL-1 β was noted after 8 and 24 h of Act treatment of cells. To confirm the Northern blot analysis data on IL-1 β induction, we performed RT-PCR analysis on total RNA from cells treated with Act. An increase in the cDNA coding for IL-1 β , which was 563 bp in size, was noted within 30 min to 2 h (data not shown), and these data matched the Northern blot data (Fig. 2). Specific primers for GAPDH were used in the same RT-PCR (used for IL-1 β) as a positive control to demonstrate that an equal amount of cDNA was used in the PCR. A dramatic increase (25-fold over control) in cDNA

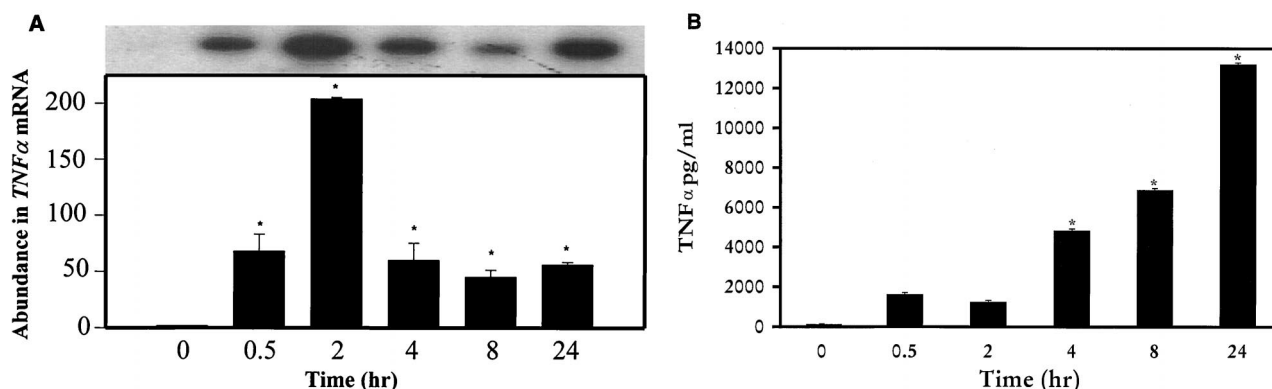


FIG. 1. Act induces TNF- α production in murine macrophages as determined by Northern blot analysis (A) and ELISA (B). (A) RAW cells were treated with 6 ng of Act/ml for the indicated times, and the supernatant was collected. The cells were dissolved in Trizol reagent for RNA isolation, and 20 μ g of total RNA was loaded onto the 3% formaldehyde gel. After transfer to a nylon membrane, the blot was probed with a murine TNF- α probe, as described in Materials and Methods. The blot was stripped and reprobed with GAPDH as an internal control to normalize the load of RNA in each lane of the gel. The blot was subjected to densitometric scanning, and the fold abundance of TNF- α mRNA was plotted. (B) The supernatant from Act-treated RAW cells at different time points was examined by ELISA for the presence of the TNF antigen. Six independent experiments were performed, and arithmetic means with standard errors were plotted. Asterisks, statistically significant differences compared to 0-h control at the $P < 0.05$ level using Scheffe's test.

for IL-6 (638 bp) was noted at 2 h by RT-PCR when macrophages were treated with Act (Fig. 3A), although an apparent increase in the IL-6 cDNA was noted within 30 min. Based on an ELISA, the IL-6 antigen level exhibited an increase at 2 h, which became maximal at 8 h (1,400 pg/ml) (Fig. 3B). Act-treated RAW cells also exhibited an increased abundance of iNOS mRNA as determined by Northern blot analysis. The mRNA for iNOS was first detected at 4 h and continued to increase for up to 24 h (Fig. 4).

The amount of LPS detected in the purified Act preparation was 0.01 ng/ml in 600 μ g of Act/ml, as determined by the *Limulus* amoebocyte lysate assay. Since the toxin was diluted to a concentration of 6 ng/ml in these experiments, the amount of LPS was negligible and thus did not contribute to these increases in proinflammatory cytokines. In a parallel set of experiments, we determined that at least 20 ng of LPS/ml was needed to cause similar increases in the TNF- α and IL-1 β

levels (data not shown), as shown for Act. LPS at a concentration of 0.0001 pg/ml present in 6 ng of Act/ml did not increase cytokine levels in RAW cells. Further, treatment of Act with polymyxin B sulfate, an antibiotic which binds LPS and inhibits its biological effects, did not alter Act's ability to induce TNF- α and IL-1 β production. On the contrary, the levels of these proinflammatory cytokines were significantly decreased (90 to 95%) in polymyxin B-treated LPS preparations at a tested concentration of 20 ng/ml (data not shown). Polymyxin B at this concentration was not toxic to the cells.

Act induces production of prostaglandins in macrophages.

We noted that the levels of PGE₂ in the supernatants of Act-treated macrophages (RAW264.7) were elevated at 4 h, becoming maximal (325 pg/ml) at 24 h, as determined by ELISA (Fig. 5). This increase in PGE₂ level was coupled to the induction of COX-2 enzyme, which produced prostaglandins from AA via the COX pathway. Based on Northern blot analysis, the abundance of *cox-2* mRNA was approximately 40-fold higher at 4 h than that of controls and gradually decreased at 8 and 24 h (Fig. 6). The level of COX-2 antigen significantly increased at 8 h, becoming maximal at 24 h, based on Western blot analysis using COX-2-specific antibodies (Fig. 6). To demonstrate that the increase in PGE₂ level indeed was coupled to the induction of COX-2 enzyme, we used specific COX-2 inhibitors NS398 and Celebrex at a concentration of 0.5 μ M. As is evident from Fig. 7, when added 1 h prior to Act, these two inhibitors abrogated PGE₂ production (98%) at the tested time point of 24 h. Cells treated with inhibitor alone did not alter basal PGE₂ levels and served as a negative control. A significant increase in the level of PGE₂ was detected in cells treated with Act alone and served as a positive control.

We then evaluated the role of PLA₂, which might be coupled to COX-2-induced PGE₂ production in Act-treated RAW cells. Based on Northern blot analysis, it was noted that Act increased the level of group V secretory PLA₂ mRNA, which became maximal at 24 h (data not shown). These data were consistent with the increase in PLA₂ activity in Act-treated RAW cells (Fig. 8A). An increase in PLA₂ activity was noted at 10 min, and activity continued to increase up to 24 h. Pre-treatment of RAW cells with sPLA₂ inhibitor LY311727 (25 μ M) for 1 h before Act addition reduced the PGE₂ production

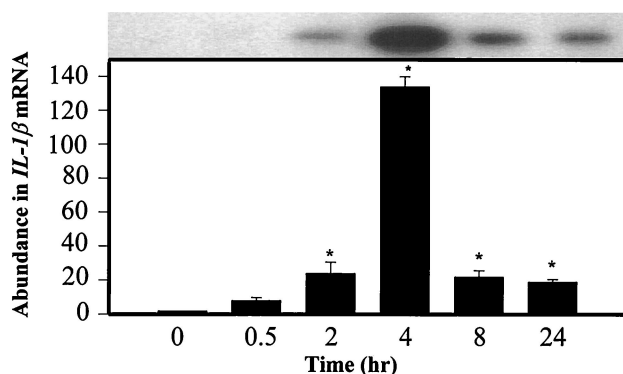


FIG. 2. Act induces IL-1 β production in murine macrophages as determined by Northern blot analysis. RAW cells were treated with 6 ng of Act/ml for the indicated times, and the cells were dissolved in Trizol reagent for RNA isolation. An aliquot (20 μ g) of total RNA was loaded onto the 3% formaldehyde gel. After transfer to a nylon membrane, the blot was probed with a murine IL-1 β probe as described in Materials and Methods. The blot was stripped and reprobed with GAPDH as an internal control to normalize the RNA load in each lane of the gel. The blot was subjected to densitometric scanning, and the fold abundance of IL-1 β mRNA was plotted. Six independent experiments were performed, and arithmetic means with standard errors were plotted. Asterisks, statistical significance at the level of $P < 0.05$ using Scheffe's test.

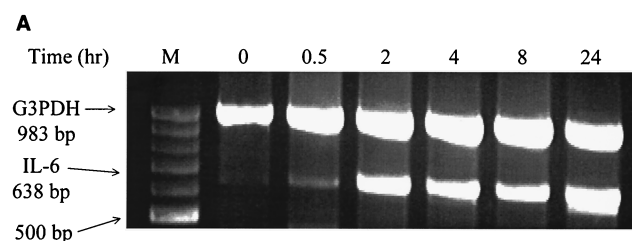
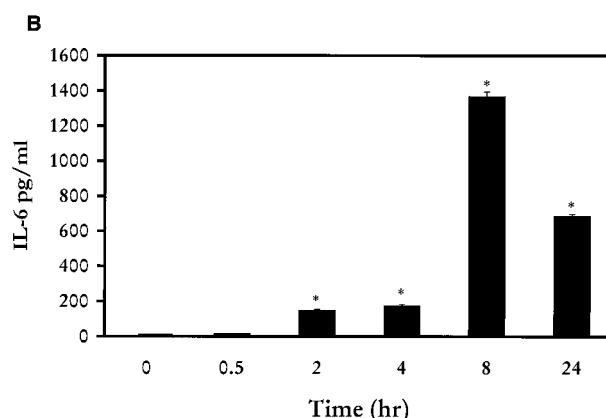


FIG. 3. Act induces production of IL-6 in murine macrophages as determined by RT-PCR (A) and ELISA (B). (A) RAW cells were treated with 6 ng of Act/ml for the indicated times, and the cells were dissolved in Trizol reagent for RNA isolation. Reverse transcription was performed on total RNA (1 μ g) as described in Materials and Methods. Subsequently, PCR was conducted on cDNA using specific primers to IL-6 and GAPDH (G3PDH) in the same reaction mixture before examining the cDNA fragments on a 0.8% agarose gel. (B) ELISA of the supernatant from Act-treated RAW cells at different time points for the presence of the IL-6 antigen. Three independent experiments were performed, and arithmetic means with standard errors were plotted. Asterisks, statistical significance at the level of $P < 0.05$ using Scheffe's test.



by 70%, which clearly indicated a role for group V sPLA₂ in Act-induced PGE₂ production (Fig. 8B).

Act induces cAMP production in macrophages. We tested whether Act would increase cAMP levels in RAW cells. As is evident in Fig. 9, cAMP levels were increased marginally in culture supernatants of Act-treated cells starting at 30 min and levels increased for up to 24 h. However, cAMP levels increased to a greater extent when the cells were treated with Act in a medium containing 0.05 mM isobutylmethylxanthine (a phosphodiesterase inhibitor), which prevented cAMP degradation. These data indicated that the fluid secretory responses observed in animal models with Act could in part be attributed to production of PGE₂ and cAMP as a result of infiltration and activation of macrophages. Indeed, rat ligated intestinal loops injected with 200 ng of Act contained four- to fivefold-elevated PGE₂ levels in the fluid. The level of PGE₂ detected in PBS-treated loops was 408 ± 21 pg/mg of protein, which increased to $2,019 \pm 58$ pg/mg of protein in loops challenged with Act. We were unable to measure accurately the cAMP in the mucosal tissue and fluid because of extensive tissue damage and marked cAMP degradation.

Act causes activation of NF- κ B and CREB transcription factors in macrophages. It is evident from Fig. 10A that Act caused an increase in nuclear translocation of a protein capable of binding a radiolabeled NF- κ B binding sequence, as determined by gel shift assay. An increase in the amount of p50 homodimer of NF- κ B was evident at 2 h (three- to fivefold

over basal level; Fig. 10A, lane 6) and remained constant up to 8 h and decreased at the 24-h time point (Fig. 10A, lanes 3 to 9). In fact the presence of a heterodimer of p50 and p65 could be visualized within 30 min (Fig. 10A, lane 5). Addition of an unlabeled NF- κ B oligonucleotide consensus primer to the nuclear extracts before adding the ³²P-labeled NF- κ B oligonucleotide blocked the binding of the latter to the NF- κ B transcription factor, indicating the specificity of the primer binding (Fig. 10A, lanes 11 and 12). Nuclear extract from HeLa cells was used as a positive control (Fig. 10A, lanes 2 and 10). The reaction mixture without the HeLa cell nuclear extract was used as a negative control in these experiments, and no radioactive band was detected (Fig. 10A, lane 1). Use of p50 antibodies caused the p50 homodimer to supershift in Act-treated cells (Fig. 10A, lane 13), further indicating the specificity of the oligonucleotide used. Lane 13 was exposed for a longer period of time to clearly demonstrate the supershifting of the p50 homodimer. Further, the p50-p65 heterodimer band disappeared using p50 antibodies (Fig. 10A, lane 13); however, the intensity of the p50-p65 supershift band was very weak (Fig. 10A, lane 13). We believe that the higher-molecular-weight band in Act-treated nuclear extract, which reacted with the labeled NF- κ B consensus oligonucleotide, represented the p50-p65 heterodimer, since the size of this band was similar to that seen in HeLa cell nuclear extract, which was used as a positive control in this experiment (Fig. 10A, lane 2). We clearly demonstrated supershifting of both the p50 homodimer and the p50-p65 heterodimer using p50 antibodies in HeLa cell

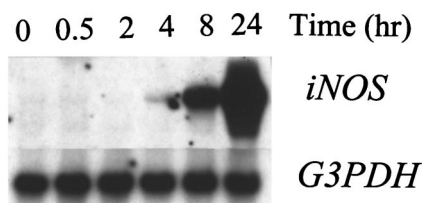


FIG. 4. Act induces the transcription of iNOS. RAW cells were treated with 6 ng of Act/ml for the indicated times and were dissolved in Trizol reagent for RNA isolation. An aliquot (20 μ g) of total RNA was loaded onto the 3% formaldehyde gel. After transfer to a nylon membrane, the blot was probed with iNOS cDNA as described in Materials and Methods. The blot was stripped and reprobed with GAPDH (G3PDH) as an internal control to normalize the RNA load in each lane of the gel. The blot was subjected to densitometric scanning, and the fold abundance of iNOS mRNA was plotted. Three independent experiments were performed, and typical Northern blot data are shown.

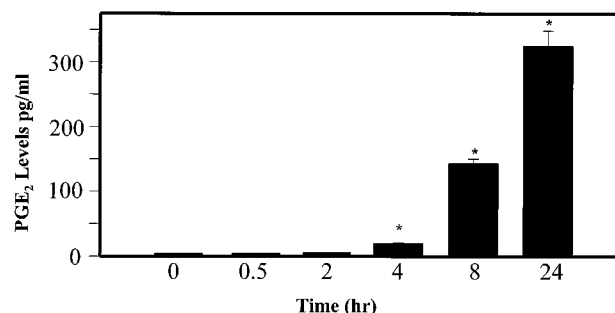


FIG. 5. Act (6 ng/ml) induces production of PGE₂. Macrophage cells were treated with Act for various times, and the supernatant was collected. The PGE₂ levels in the supernatant were determined by enzyme immunoassay as described in Materials and Methods. Asterisks, statistically significant differences at $P < 0.05$ compared to 0-h control from four independent experiments.

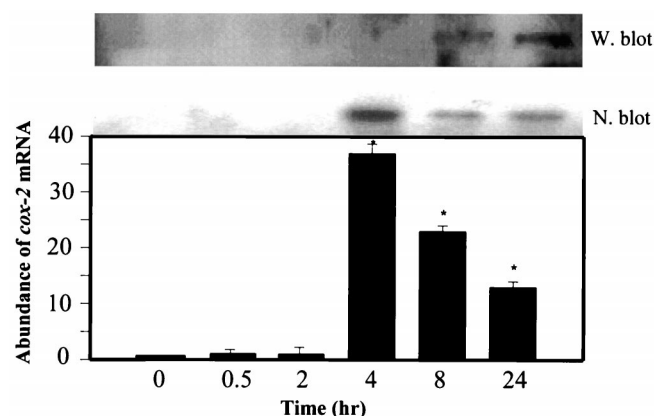


FIG. 6. Act induces COX-2 production. (N. blot). RAW cells were treated with 6 ng of Act/ml for the indicated times and were dissolved in Trizol reagent for RNA isolation. An aliquot (20 μ g) of total RNA was loaded onto the 3% formaldehyde gel. After transfer to a nylon membrane, the blot was probed with *cox-2* cDNA. The blot was stripped and reprobed with GAPDH as an internal control to normalize the RNA load in each lane of the gel. The blot was subjected to densitometric scanning, and the fold abundance of *cox-2* mRNA (arithmetic means with standard errors) were plotted. Three independent experiments were performed. Asterisks, statistical significance at the $P < 0.05$ level using Scheffe's test. (W. blot). Proteins (50 μ g) from RAW cells treated with Act for various times were loaded onto an SDS-12% polyacrylamide gel and subjected to Western blot analysis using affinity-purified goat polyclonal antibodies to a peptide (amino acid residues 27 to 46) representing the amino-terminal end of rat COX-2. These antibodies react with rat, mouse, and human COX-2. The secondary antibodies (rabbit anti-goat antibody diluted 1:30,000) conjugated with HRP were used, and the blot was developed with enhanced chemiluminescence substrate.

nuclear extract which contained abundant amounts of the p50 homodimer and the p50-p65 heterodimer (Fig. 10A, lane 15). Similarly, antibodies to p65 caused supershifting of the p50-p65 heterodimer in HeLa cell nuclear extract (Fig. 10A, lane 14).

In a similar experiment, a cAMP-responsive element (CRE) binding protein (CREB)-specific consensus primer was used in the gel shift assay. We noted that proteins from nuclear extracts from Act-treated RAW cells bound to the 32 P-labeled CREB-specific primer (Fig. 10B, lanes 2 to 8). The increase in CREB was apparent at 2 h. Once again, a reaction mixture

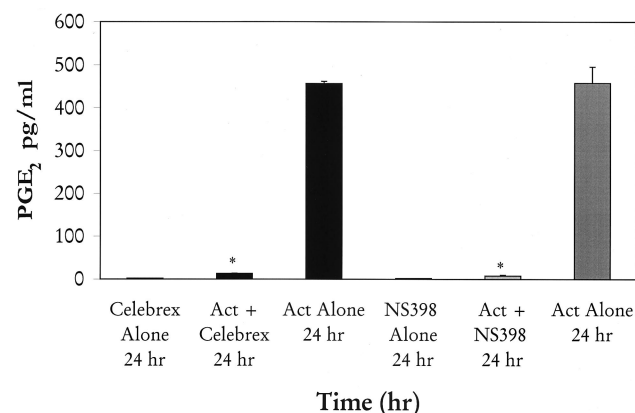


FIG. 7. Act-induced PGE₂ production is inhibited by COX-2-specific inhibitors. COX-2 inhibitors NS398 and Celebrex were added at a 0.5 μ M concentration 1 h before adding Act (6 ng/ml) to RAW cells. The PGE₂ level in the supernatant was monitored after 24 h. Three independent experiments were performed, and arithmetic means with standard errors were plotted. Asterisks, statistical significance at $P < 0.05$ compared to control using Scheffe's test.

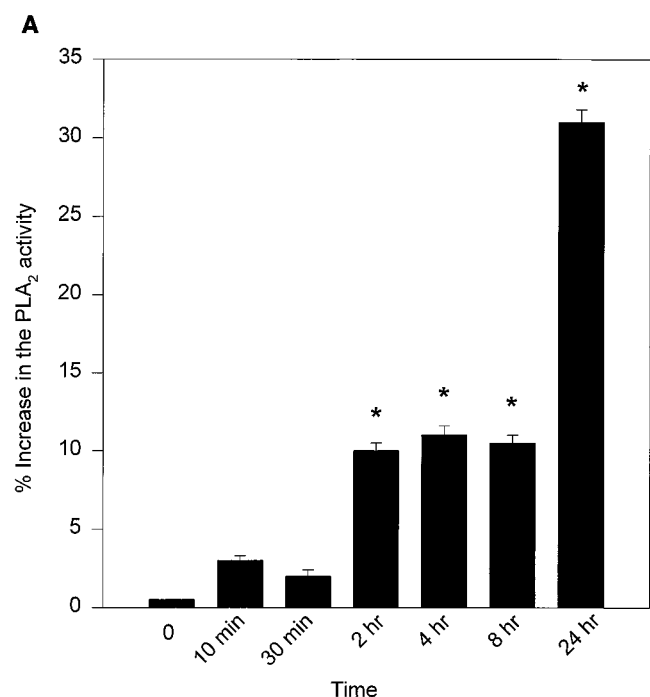
without HeLa cell nuclear extract served as a negative control (Fig. 10B, lane 1). The specificity of labeled CREB oligonucleotide to bind to CREB protein was confirmed by competition with a non-radioactively labeled CREB oligonucleotide (Fig. 10B, lanes 9 to 11). Likewise, the intensity of the CREB-specific band at the 24-h time point after Act treatment decreased dramatically when CREB antibodies were used (Fig. 10B, lane 12). The detection of weaker supershift bands could be due to the binding of NF- κ B and CREB antibodies to a region to which specific oligonucleotides bind, thus preventing efficient binding of radiolabeled oligonucleotides to NF- κ B or CREB. Alternatively, concentration of the commercial antibodies or the amount of NF- κ B or CREB in Act-treated cells might not be high enough to clearly show supershift bands. No activation of other transcription factors, such as AP-1, AP-2, SP-1, TFIID, or OCT-1, was noted, indicating that Act specifically activated NF- κ B and CREB.

Act induces antiapoptotic protein Bcl-2 in macrophages. Treatment of macrophages with Act caused upregulation of the antiapoptotic protein Bcl-2, which was maximally (five- to eightfold increase over control) detected at 4 h (Fig. 11). Bcl-2 could prevent massive apoptosis of cells resulting from the production of proinflammatory cytokines induced by Act and may represent a host defense against cell death.

DISCUSSION

Act and other extracellular enzymes produced by *Aeromonas* spp. are important virulence factors involved in the pathogenesis of *Aeromonas* infections (14, 52, 69). Act has multiple biological activities, ranging from its ability to cause extensive tissue injury to its evocation of a fluid secretory response in ligated small intestinal loops of animals. The present study was undertaken to examine which Act-induced proinflammatory cytokines might lead to pathogenic effects in animals. Indeed, evidence that many bacterial toxins possess cytokine-inducing activities is accumulating (30, 31), and therefore the host proinflammatory cytokine response to Act may contribute to the pathogenesis of *Aeromonas* infections. Further, it was intriguing to determine a mechanism by which Act evoked PGE₂ and cAMP production, which could lead to fluid secretion in animals. To dissect Act's mechanism of action, we opted to use murine macrophage cell line RAW264.7. The Act concentration selected was 6 ng/ml, which did not affect the viability of these cells. Our studies also were designed to clarify intracellular signaling mechanisms involved in (i) toxin induction of cytokine gene expression and (ii) Act-induced expression of the *cox-2* gene involved in PGE₂ production through activation of transcription factors.

Our results demonstrated that Act caused increased levels of proinflammatory cytokines, such as TNF- α , IL-1 β , and IL-6, as determined by Northern blot analysis, RT-PCR, and ELISA (Fig. 1 to 3). We demonstrated that the increased levels of these cytokines were Act specific, as the LPS contamination in the purified preparation of Act was negligible. Further, we noted that treatment of Act with polymyxin B sulfate did not alter the toxin's ability to induce production of various cytokines. We also noted that peritoneal macrophages derived from an LPS-hyporesponsive mouse strain (C3H/HeJ) responded to Act and produced various proinflammatory cytokines, whereas LPS at a tested concentration of 20 ng/ml did not elevate TNF- α and IL-1 β levels in these macrophages. While our studies were in progress, Braun et al. (10) reported that pneumolysin, a pore-forming hemolysin produced by *Streptococcus pneumoniae*, also was capable of increasing TNF- α and IL-6 levels in macrophages. Like Act, pneumolysin



binds to cholesterol and forms large oligomeric pores (60). Shiga toxin from *Shigella dysenteriae* inhibits protein synthesis and similarly increases proinflammatory cytokine production (TNF- α , IL-1 β , and IL-6) in macrophages. However, Shiga toxin selectively targets vascular endothelial cells (65).

Act-mediated induction of iNOS (Fig. 4) possibly occurs via upregulation of TNF- α and IL-1 β in the host cell. Nitric oxide (NO) production by iNOS is an essential element of antimicrobial immunity and host-induced tissue damage (10). Since *Aeromonas* spp. cause invasive diseases, this report represents the first study showing that a protein toxin in *Aeromonas* is responsible for iNOS production. Recently, the leukotoxin produced by *Pasteurella haemolytica*, a member of the repeats-in-toxin family of pore-forming exotoxins, has been shown to induce gene expression for iNOS in bovine alveolar macrophages (34). It has been shown that the mechanism of iNOS regulation involves IFN- γ -mediated upregulation of IFN regulatory factor 1 (IRF-1) expression. IRF-1 binds to the iNOS promoter and activates iNOS transcription synergistically with NF- κ B, induced through TNF, IL-1, or LPS signaling (39, 68). Recent studies of Braun et al. (10) indicated that RAW cells could synthesize enough endogenous IFN- γ within cultures to activate iNOS expression when exposed to pneumolysin from *S. pneumoniae*, which also could be the case with Act-stimulated RAW cells. In contrast, iNOS expression by LPS and TNF is normally dependent on IFN- γ signaling and requires priming with exogenous IFN- γ (10).

Act caused macrophages to release PGE₂ in the supernatant, and the production of this eicosanoid was abrogated by COX-2 inhibitors (NS398 and Celebrex) (Fig. 5 and 7). These data indicated that Act induced production of PGE₂ from AA via a COX pathway (54). Since AA is present at a limited concentration in the cells, we demonstrated that Act elevated cellular levels of AA by increasing the expression of group V sPLA₂, which acted on the membrane phospholipids of eukaryotic cells (Fig. 8A). Recently, a similar upregulation of group V sPLA₂ by LPS in macrophages was reported (8). Our data with regard to the role of group V sPLA₂ in regulating PGE₂ production in Act-treated RAW cells were substantiated further,

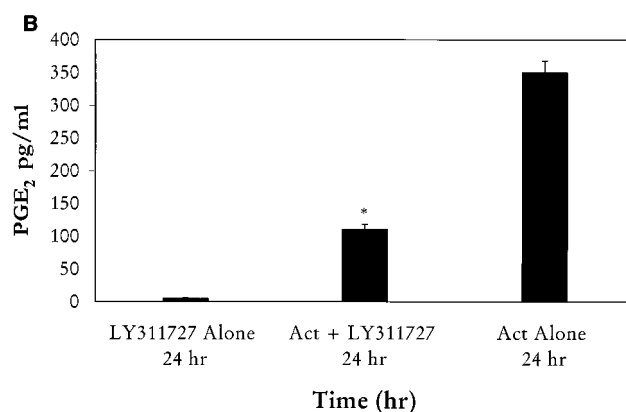


FIG. 8. (A) Act (6 ng/ml) increases PLA₂ activity in macrophages. The supernatants from Act-treated RAW cells were tested for PLA₂ activity using [³H]AA-labeled *E. coli* cells as described in Materials and Methods. Averages from four experiments were plotted with standard errors. (B) An inhibitor of sPLA₂ reduces PGE₂ levels in macrophages. Group II and V sPLA₂ inhibitor LY311727 (25 μ M) was added at 1 h before adding Act to RAW cells. The PGE₂ level in the supernatant was monitored after 24 h. Three independent experiments were performed, and arithmetic means with standard errors were plotted. Asterisks, statistical significance ($P < 0.05$) compared to 0-h control using Scheffe's test.

as a specific inhibitor of sPLA₂ (both groups II and V) dramatically reduced PGE₂ production in RAW cells (Fig. 8B). We have shown that LPS stimulated the production of group II sPLA₂ in murine macrophages, as determined by Western blot analysis (unpublished data). However, Act failed to induce group II sPLA₂ production but caused increased expression of the group V PLA₂-encoding gene. Increased sPLA₂ at the surfaces of activated cells is due to gene induction and de novo protein synthesis and not due to exocytosis of preformed protein (8). Our earlier studies indicated that actinomycin D and cycloheximide inhibited cholera toxin (CT)-induced fluid secretion in rabbit ligated small intestinal loops, indicating a role for de novo protein synthesis in the mechanism of action of CT (54). Subsequently, we demonstrated that CT upregulated in both epithelial cell lines and macrophages a gene encoding PLA₂-activating protein (PLAA), which exhibited homology with numerous G-protein β -subunits (51, 54). PLAA has been

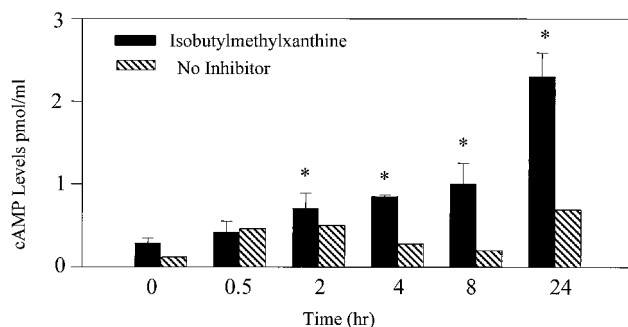


FIG. 9. Act (6 ng/ml) increases cAMP production in macrophages. The supernatants from Act-treated RAW cells were tested for increased levels of cAMP using ELISA (see Materials and Methods). The experiment was performed in the absence (hatched bar) or presence (solid bar) of isobutylmethylxanthine (0.05 mM), which is a phosphodiesterase inhibitor. Averages from three independent experiments with standard deviations were plotted. Asterisks, statistically significant difference ($P < 0.05$) compared to the 0-h control.

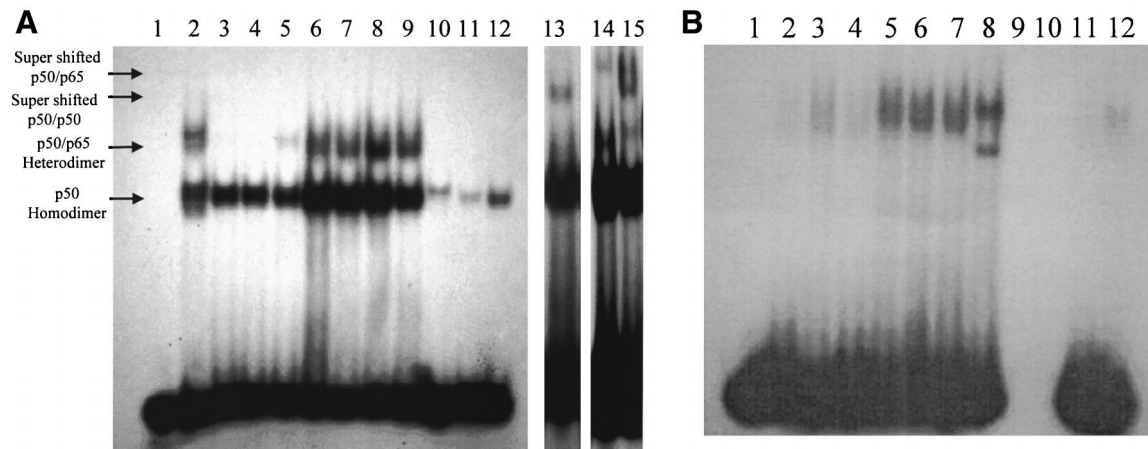


FIG. 10. Act (6 ng/ml) activates NF- κ B and CREB transcription factors in RAW cells as determined by gel shift and supershift assays. Nuclear extracts (10 μ g) from Act-treated RAW cells were mixed with consensus primers for NF- κ B and CREB, subjected to a nondenaturing 4% polyacrylamide gel electrophoresis (see Materials and Methods), and autoradiographed. (A) Nuclear extracts from HeLa and Act-treated RAW cells at the time points indicated below were examined for NF- κ B. Lane 1, no HeLa cell extract (negative control); lane 2, with HeLa cell extract (positive control); lanes 3 to 9, nuclear extract from Act-treated RAW cells at 0, 10, and 30 min and at 2, 4, 8, and 24 h, respectively; lane 10, nuclear extract from HeLa cells mixed with a cold consensus primer before adding the radioactive primer; lane 11, nuclear extract from Act-treated RAW cells mixed with a cold consensus primer before adding the radioactive primer (0 h); lane 12, 24-h sample; lane 13, supershift assay using antibodies to p50 with Act-treated RAW cells; lanes 14 and 15, supershift assays with HeLa cell nuclear extract using antibodies to p65 (lane 14) and p50 (lane 15). Free [32 P]dCTP runs at the bottom of the gel. (B) Nuclear extracts from HeLa and Act-treated RAW cells at the time points indicated below were examined for CREB. Lane 1, no HeLa cell extract (negative control); lanes 2 to 8, nuclear extract from Act-treated RAW cells at 0, 10, and 30 min and at 2, 4, 8, and 24 h, respectively; lane 9, nuclear extract from HeLa cells mixed with a cold consensus primer before adding the radioactive primer; lane 10, nuclear extract from Act-treated RAW cells mixed with a cold consensus primer before adding the radioactive primer (0 h); lane 11, 24-h sample; lane 12, antibodies to CREB were added before radiolabeled CREB-specific primer. Three to five independent experiments were performed, and data from a typical experiment are shown.

shown to upregulate the expression of group II sPLA₂ in murine BC3H1 cells (21). Therefore, we tested whether Act would activate group V sPLA₂ in macrophages as well via PLAA. However, our Northern blot analysis demonstrated that Act did not alter the expression of the gene encoding PLAA, suggesting thereby a different mechanism of activation of group V sPLA₂ by Act, which is under investigation. Interestingly, LPS induced the production of PLAA in macrophages (data not shown). Our data indicated for the first time that Act-induced PGE₂ production was linked to the COX-2 pathway and is, in turn, coupled to group V sPLA₂. We noted that the kinetics of Act-induced *cox-2* gene expression in macrophages (Fig. 6) was different from that in cells exposed to LPS. The mRNA for *cox-2* was short-lived, as its level declined after 4 h of treatment of macrophages with Act. However, LPS-induced *cox-2* mRNA was stable up to 24 h (data not shown). Taken together, these data indicated that Act induced the production of proinflammatory cytokines (TNF- α , IL-1 β , and IL-6) as well as iNOS in macrophages. It is therefore plausible that these inflammatory mediators cause the extensive tissue injury seen in ligated intestinal loops of experimental animals challenged with Act. We also have demonstrated that Act increases TNF- α levels in intestinal epithelial cell line IEC-6 (data not shown). TNF- α loosens the tight junctions around epithelial cells allowing (i) influx of inflammatory cells into the intestinal lumen and (ii)

increased uptake of Act into the lamina propria, where inflammatory cells could be activated (49). At present, we are investigating whether the extent of inflammation induced by Act in ligated intestinal loops correlates with the fluid secretory response.

We also demonstrated that Act increased cAMP production in macrophages (Fig. 9), which could occur as a result of (i) direct activation of G-protein-coupled adenylate cyclase or (ii) indirect activation of adenylate cyclase by PGE₂ (54). It also is known that PGE₂ induces adenylate cyclase, which forms cAMP from ATP (53). Both cAMP and PGE₂ production by macrophages may in part be responsible for evoking fluid secretion in animals by Act (53) as a result of infiltration and activation of macrophages. Our recent data suggested that most of the cAMP was produced through PGE₂ activation of the adenylate cyclase enzyme. We noted that treatment with Celebrex or sPLA₂ inhibitor, which dramatically reduced Act-induced PGE₂ production (Fig. 7 and 8B), significantly decreased cAMP levels (70 to 80%) in Act-treated RAW cells. The remainder of the cAMP might have been generated through direct activation of adenylate cyclase enzyme. However, the adenylate cyclase activity should be measured in Act-treated cells to draw a firm conclusion.

Our results indicated that Act caused an increase in the nuclear translocation of proteins capable of binding NF- κ B and CREB-binding sequences within the first 2 h (Fig. 10). Transcription factor NF- κ B is important in a number of inflammation-related pathways (63), and binding elements for the transcriptional regulatory factors NF- κ B and CREB are present in the enhancer/promoter regions of immunoregulatory cytokine genes, including the TNF- α , IL-1 β , and IL-6 genes. These transcription factors have important functions in modulating the transcription of cytokine and *cox-2* genes, as well as of cellular adhesion molecules (27, 63, 67). An inactive NF- κ B heterodimer which consists of p50 and p65 subunits is

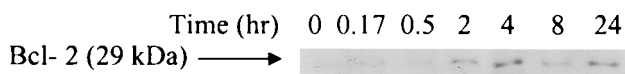


FIG. 11. Western blot analysis showing that Act (6 ng/ml) increases Bcl-2 levels in macrophages. An aliquot of cellular proteins (50 μ g) at different time points after Act treatment was loaded on an SDS-12% polyacrylamide gel and subjected to Western analysis as described in Materials and Methods. The blot was developed using an ECL kit. Three independent experiments were performed.

present in the cytoplasm in complex with inhibitory protein I- κ B, which binds NF- κ B in the cytoplasm and prevents its translocation to the nucleus (34). NF- κ B activation results in phosphorylation, ubiquitination, and degradation of I- κ B, leading to nuclear translocation of NF- κ B and its binding to specific enhancer/promoter sequences, resulting in expression of target genes. Our data indicated that Act mediated the selective upregulation of transcription in macrophages by inducing intracellular signaling events, resulting in nuclear translocation of transcriptional activators NF- κ B and CREB (Fig. 10). Interestingly, we noted the translocation of the p50 homodimer of NF- κ B in the nucleus of RAW cells even at 0 h, and translocation increased after Act treatment (Fig. 10A). Recently, it has been reported that translocation of the p50 homodimer in the nucleus may be important to prevent upregulation of genes encoding proinflammatory cytokines in unstimulated cells (40). Therefore, the p50 homodimer may prevent overactivation of the proinflammatory cytokines by the p50-p65 heterodimer of NF- κ B. Recently, leukotoxin produced by *P. haemolytica* was reported to cause translocation of nuclear NF- κ B after a 5-min exposure in bovine alveolar macrophages, as measured by immunofluorescence using confocal microscopy (34). It was noted further that bovine alveolar macrophages pretreated with an inhibitor of tyrosine kinases (e.g., herbimycin A) did not cause activation of NF- κ B by leukotoxin, indicating that tyrosine phosphorylation was required for leukotoxin-induced NF- κ B activation. It needs to be determined whether protein kinases play a role in Act-mediated signaling. It is particularly important, as herbimycin A did not affect either TNF- α and IL-8 gene expression or NF- κ B activation in LPS-induced bovine alveolar macrophages, indicating the involvement of the tyrosine kinase-insensitive LPS-signaling pathway or the involvement of another transcription factor(s) in the expression of TNF and IL-8. Interestingly, it has been suggested that expression of the TNF- α gene is down-regulated by agents that elevate cAMP (e.g., PGE₂, dibutyryl cAMP, CT, and 8-bromo-cAMP), with a concomitant decrease in protein kinase A activity (64). It is therefore possible that the reduced mRNA levels of TNF- α in Act-treated macrophages after 2 h might be due to (i) the short half-life of TNF- α mRNA and (ii) an increase in cAMP in cells treated with Act (Fig. 1A and 9). A continuous increase in the TNF- α antigen level up to 24 h may be reflected by the translation of the existing TNF transcript in the cells (Fig. 1B).

Interestingly, NF- κ B activation induced by hypoxia remained unaffected in epithelial cells exposed to 8-bromo-cAMP, and the role of CRE and CRE-binding proteins (CREB) in inducing TNF- α in hypoxia has been reported (64). The CREB family of transcription factors are leucine zipper proteins that bind to the CRE with the consensus sequence 5'-TGACGTCA-3' (64). CREB is phosphorylated at serine 133 by protein kinase A in response to cAMP, and this leads to transcriptional activation of genes with promoters containing the CRE sequence. Other signaling pathways that lead to phosphorylation and CREB activation include calmodulin kinase, which phosphorylates CREB in response to increased intracellular Ca²⁺, and protein kinase Rsk2 (a member of the pp90 ribosomal protein S6 kinase family), which is activated by mitogen-activated protein kinases (64). Whether Act activates CREB through the above-mentioned signaling pathways needs to be determined. Hsuan et al. (34) reported that elevation of intracellular Ca²⁺ in leukotoxin-stimulated bovine alveolar macrophages was essential for NF- κ B activation and cytokine gene expression, as chelation of intracellular Ca²⁺ blocked both of these responses. These studies are very provocative, since NF- κ B recently was shown to induce CREB promoter

activity in Sertoli and NIH 3T3 cells (22). Studies of Krause et al. (42) indicated that aerolysin, which exhibited homology with Act, increased intracellular Ca²⁺ levels in human granulocytes (HL-60). Therefore, these toxins could plausibly require Ca²⁺ for both NF- κ B and CREB activation.

Act-induced expression of the gene encoding COX-2 led to increased PGE₂ production in RAW cells (Fig. 5 and 6). Recently, Wang and Tai (67) suggested that CRE might mediate the induction of prostaglandin H synthase-2 (COX-2) expression in human amnion-derived WISH cells. These studies correlate with our findings that the *cox-2* gene expression might be linked to the CREB activation (Fig. 5 and 10B). We believe that both NF- κ B and CREB might be involved in the *cox-2* gene expression induced by Act, because two NF- κ B binding sites have been shown to be present at positions -265 and -490 upstream of the *cox-2* gene (4) and Act-activated NF- κ B (Fig. 10A). Further, there is one CRE site at position -101 upstream of the *cox-2* gene (4). Recent studies of Abate et al. (1) indicated that SN50, an inhibitor of NF- κ B translocation, indeed attenuated PGE₂ accumulation in culture supernatants of LPS-stimulated macrophages. It needs to be determined whether Act phosphorylates Rsk2, resulting in activation of transcription factor CREB. Interestingly, LPS has been shown to activate AP-1 (27); however, Act did not affect AP-1 or other transcription factor levels in RAW cells.

Our studies also indicated that Act generated antiapoptotic signals in Act-treated macrophages (Fig. 11). Our data are consistent with the recent findings that NF- κ B protected cells against TNF-induced cell death by inducing the expression of antiapoptotic genes (71). Thus, the host responses are triggered by Act to prevent cell death, which is beneficial for the bacteria. However, the extent of host tissue injury is determined by the number of bacteria during infection and the amount of Act secreted by *Aeromonas*. It is not known whether PLA₂ also triggers antiapoptotic signals (e.g., Bcl-2) in cells. It is plausible that high levels of sPLA₂ accumulated at inflammatory sites by Act may not only regulate inflammation but also protect cells from unnecessary death induced by proinflammatory agents as a result of production of antiapoptotic proteins. It is also possible that activation of CREB by Act might enhance the expression of the gene encoding Bcl-2. In this context, it is interesting to note that insulin-like growth factor-I induces antiapoptotic protein Bcl-2 through the nuclear transcription of CREB in PC12 cells employing a novel signaling pathway involving MAPK 6, p38 β MAPK, and MAPKAP-K3, resulting in the induction of the *bcl-2* promoter containing the CRE binding site (57). It is therefore tempting to speculate that Act may operate through a similar pathway, as CREB levels are increased in macrophages treated with Act (Fig. 10B). Further studies on signal transduction in Act-treated macrophages are in progress.

In conclusion, Act upregulates the production of proinflammatory cytokines and antiapoptotic protein Bcl-2 as well as activates AA metabolism in macrophage/monocyte cells. The increased expression of genes encoding proinflammatory cytokines, Bcl-2, and COX-2 appears related to activation of transcription factors NF- κ B and CREB. Act-induced PGE₂ production has been linked to upregulation of COX-2, which is coupled to group V sPLA₂. This is the first report of a detailed mechanism of action of Act from *A. hydrophila*. Further studies on Act-induced signal transduction in macrophages would elicit pathogenic sequelae associated with *Aeromonas* infections.

ACKNOWLEDGMENTS

This work was supported by Public Health Service grant AI41611 from the National Institutes of Health.

We thank Madelle Susman for editorial comments and Lyska Morrison for secretarial help.

REFERENCES

- Abate, A., S. Oberle, and H. Schroder. 1998. Lipopolysaccharide-induced expression of cyclooxygenase-2 in mouse macrophages is inhibited by chloromethylketones and a direct inhibitor of NF- κ B translocation. *Prostaglandins Other Lipid Mediat.* **56**:277–290.
- Abbott, S. L., L. S. Seli, M. Catino, Jr., M. A. Hartley, and J. M. Janda. 1998. Misidentification of unusual *Aeromonas* species as members of the genus *Vibrio*: a continuing problem. *J. Clin. Microbiol.* **36**:1103–1104.
- Altwegg, M., L. G. Martinetti, J. Luthy-Hottenstein, and M. Rohrbach. 1991. *Aeromonas*-associated gastroenteritis after consumption of contaminated shrimp. *Eur. J. Clin. Microbiol. Infect. Dis.* **10**:44–45.
- Appleby, S. B., A. Ristimäki, K. Neilson, K. Narko, and T. Hla. 1994. Structure of human cyclo-oxygenase-2 gene. *Biochem. J.* **302**:723–727.
- Asao, T., Y. Kinoshita, S. Kozaki, T. Uemura, and G. Sakaguchi. 1984. Purification and some properties of *Aeromonas hydrophila* hemolysin. *Infect. Immun.* **46**:122–127.
- Atkinson, H. M., and T. J. Trust. 1980. Hemagglutination properties and adherence ability of *Aeromonas hydrophila*. *Infect. Immun.* **27**:938–946.
- Ausubel, F. M., R. Brent, R. E. Kingston, D. D. Moore, J. G. Seidman, J. A. Smith, and K. Struhl (ed.). 1989. Current protocols in molecular biology. John Wiley and Sons, Inc., New York, N.Y.
- Balboa, M. A., J. Balsinde, M. V. Winstead, J. A. Tischfield, and E. A. Dennis. 1996. Novel group V phospholipase A₂ involved in arachidonic acid mobilization in murine P388D₁ macrophages. *J. Biol. Chem.* **271**:32381–32384.
- Barnett, T. C., S. M. Kirov, M. S. Strom, and K. Sanderson. 1997. *Aeromonas* spp. possess at least two distinct type IV pilus families. *Microb. Pathog.* **23**:241–247.
- Braun, J. S., R. Novak, G. Gao, P. J. Murray, and J. L. Shenep. 1999. Pneumolysin, a protein toxin of *Streptococcus pneumoniae*, induces nitric oxide production from macrophages. *Infect. Immun.* **67**:3750–3756.
- Buchanan, R. L., and S. A. Palumbo. 1985. *Aeromonas hydrophila* and *Aeromonas sobria* as potential food poisoning species: a review. *J. Food Safety* **7**:15–29.
- Carnahan, A. M., and M. Altwegg. 1996. The genus *Aeromonas*, p. 1–38. In B. Austin, M. Altwegg, P. J. Gosling, and S. Joseph (ed.), *Taxonomy*. John Wiley & Sons, New York, N.Y.
- Chakraborty, T., B. Huhle, H. Bergbauer, and W. Goebel. 1986. Cloning, expression, and mapping of the *Aeromonas hydrophila* aerolysin gene determinant in *Escherichia coli* K-12. *J. Bacteriol.* **167**:368–374.
- Chakraborty, T., B. Huhle, H. Hof, H. Bergbauer, and W. Goebel. 1987. Marker exchange mutagenesis of the aerolysin determinant in *Aeromonas hydrophila* demonstrates the role of aerolysin in *A. hydrophila* associated systemic infections. *Infect. Immun.* **55**:2274–2280.
- Chakraborty, T., M. A. Montenegro, S. C. Sanyal, R. Helmuth, E. Bulling, and K. N. Timmis. 1984. Cloning of enterotoxin gene from *Aeromonas hydrophila* provides conclusive evidence of production of a cytotoxic enterotoxin. *Infect. Immun.* **46**:435–441.
- Chakraborty, T., A. Schmidt, S. Notermans, and R. Benz. 1990. Aerolysin of *Aeromonas sobria*: evidence for formation of ion-permeable channels and comparison with alpha-toxin of *Staphylococcus aureus*. *Infect. Immun.* **58**:2127–2132.
- Chopra, A. K., and C. W. Houston. 1999. Enterotoxins in *Aeromonas*-associated gastroenteritis. *Microbes Infect.* **1**:1129–1137.
- Chopra, A. K., C. W. Houston, J. W. Peterson, and G. F. Jin. 1993. Cloning, expression, and sequence analysis of a cytolytic enterotoxin gene from *Aeromonas hydrophila*. *Can. J. Microbiol.* **39**:513–523.
- Chopra, A. K., C. W. Houston, and A. Kurosky. 1991. Genetic variation in related cytolytic toxins produced by different species of *Aeromonas*. *FEMS Microbiol. Lett.* **79**:231–237.
- Chopra, A. K., J. Peterson, X. J. Xu, D. H. Coppenhaver, and C. W. Houston. 1996. Molecular and biochemical characterization of a heat-labile enterotoxin from *Aeromonas hydrophila*. *Microb. Pathog.* **21**:357–377.
- Clark, M. A., L. E. Ozgur, T. M. Conway, J. Dispoto, S. T. Crooke, and J. S. Bomalaski. 1991. Cloning of a phospholipase A₂-activating protein. *Proc. Natl. Acad. Sci. USA* **88**:5418–5422.
- Delfino, F. J., and W. H. Walker. 1999. NF- κ B induces cAMP-response element-binding protein gene transcription in Sertoli cells. *J. Biol. Chem.* **274**:35607–35613.
- Ferguson, M. R., X. J. Xu, C. W. Houston, J. W. Peterson, D. H. Coppenhaver, V. L. Popov, and A. K. Chopra. 1997. Hyperproduction, purification, and mechanism of action of the cytotoxic enterotoxin produced by *Aeromonas hydrophila*. *Infect. Immun.* **65**:4299–4308.
- Ferguson, M. R., X. J. Xu, C. W. Houston, J. W. Peterson, and A. K. Chopra. 1995. Amino-acid residues involved in biological functions of the cytolytic enterotoxin from *Aeromonas hydrophila*. *Gene* **156**:79–83.
- Gerland, W. J., and J. T. Buckley. 1988. The cytolytic toxin aerolysin must aggregate to disrupt erythrocyte membranes, and aggregation is stimulated by human glycophorin. *Infect. Immun.* **56**:1249–1253.
- Grey, P. A., and S. M. Kirov. 1993. Adherence to Hep-2 cells and enteropathogenic potential of *Aeromonas* spp. *Epidemiol. Infect.* **110**:279–287.
- Gupta, D., Q. Wang, C. Vinson, and R. Dziarski. 1999. Bacterial peptidoglycan induces CD14-dependent activation of transcription factors CREB/ATF and AP-1. *J. Biol. Chem.* **274**:14012–14020.
- Hanninen, M. L., P. Oivanen, and V. Hirvelä-Koski. 1997. *Aeromonas* species in fish, fish-eggs, shrimp and freshwater. *Int. J. Food Microbiol.* **34**:17–26.
- Hanninen, M. L., S. Salmi, L. Mattila, R. Taipalin, and A. Siitonen. 1995. Association of *Aeromonas* spp with traveller's diarrhoea in Finland. *J. Med. Microbiol.* **41**:26–31.
- Henderson, B., S. Poole, and M. Wilson. 1996. Bacterial modulins: a novel class of virulence factors which cause host tissue pathology by inducing cytokine synthesis. *Microbiol. Rev.* **60**:316–341.
- Henderson, B., M. Wilson, and B. Wren. 1997. Are bacterial exotoxins cytokine network regulators? *Trends Microbiol.* **5**:454–458.
- Howard, S. P., and J. T. Buckley. 1986. Molecular cloning and expression in *Escherichia coli* of the structural gene for the hemolytic toxin aerolysin from *Aeromonas hydrophila*. *Mol. Gen. Genet.* **204**:289–295.
- Howard, S. P., W. J. Garland, M. J. Green, and J. T. Buckley. 1987. Nucleotide sequence of the gene for the hole-forming toxin aerolysin of *Aeromonas hydrophila*. *J. Bacteriol.* **169**:2869–2871.
- Hsuan, S. L., M. S. Kannan, S. Jeyaseelan, Y. S. Prakash, C. Malazdrewich, M. S. Abrahamsen, G. C. Sieck, and S. K. Maheswaran. 1999. *Pasteurella haemolytica* leukotoxin and endotoxin induced cytokine gene expression in bovine alveolar macrophages requires NF- κ B activation and calcium elevation. *Microb. Pathog.* **26**:263–273.
- Husslein, V., B. Huhle, T. Jarchau, R. Lurz, W. Goebel, and T. Chakraborty. 1988. Nucleotide sequence and transcriptional analysis of the *AerCaeA* region of *Aeromonas sobria* encoding aerolysin and its regulatory region. *Mol. Microbiol.* **2**:507–517.
- Janda, J. M., and S. L. Abbott. 1998. Evolving concepts regarding the genus *Aeromonas*: an expanding panorama of species, disease presentations, and unanswered questions. *Clin. Infect. Dis.* **27**:332–344.
- Jin, G. F., A. K. Chopra, and C. W. Houston. 1992. Stimulation of neutrophil leukocyte chemotaxis by a cloned cytolytic enterotoxin of *Aeromonas hydrophila*. *FEMS Microbiol. Lett.* **98**:285–290.
- Jin, G. F., and C. W. Houston. 1992. The effect of *Aeromonas hydrophila* enterotoxins on the phagocytic function of mouse phagocytes. *Dig. Dis. Sci.* **37**:1697–1703.
- Kamijo, R., H. Harada, T. Matsuyama, M. Bosland, J. Gerecitano, D. Shapiro, J. Le, S. I. Koh, T. Kimura, S. J. Green, T. W. Mak, T. Taniguchi, and J. Vilcek. 1994. Requirement for transcription factor IRF-1 in NO synthase induction in macrophages. *Science* **263**:1612–1615.
- Kastenbauer, S., and H. W. Loms Ziegler-Heitbrock. 1999. NF- κ B1 (p50) is upregulated in lipopolysaccharide tolerance and can block tumor necrosis factor gene expression. *Infect. Immun.* **67**:1553–1559.
- Kirov, S. M., E. K. Ardestani, and L. J. Hayward. 1993. The growth and expression of virulence factors at refrigeration temperature by *Aeromonas* strains isolated from foods. *Int. J. Food Microbiol.* **20**:159–168.
- Krause, K. H., M. Fivaz, A. Monod, and F. G. van der Goot. 1998. Aerolysin induces G-protein activation and Ca²⁺ release from intracellular stores in human granulocytes. *J. Biol. Chem.* **273**:18122–18129.
- Ljungh, A., P. Eneroth, and T. Wadstrom. 1982. Cytotoxic enterotoxin from *Aeromonas hydrophila*. *Toxicon* **20**:787–794.
- Majeed, K. N., A. F. Egan, and I. C. MacRae. 1990. Production of exotoxins by *Aeromonas* spp. at 5°C. *J. Appl. Bacteriol.* **69**:332–337.
- Merino, S., A. Aguilar, M. M. Noguera, M. Regue, S. Swift, and J. M. Tomas. 1999. Cloning, sequencing, and role of two phospholipases (A1 and C) from mesophilic *Aeromonas* sp. serogroup O:34. *Infect. Immun.* **67**:4008–4013.
- Merino, S., M. M. Noguera, A. Aguilar, X. Rubires, S. Alberti, V. J. Benedi, and J. M. Tomas. 1998. Activation of the complement classical pathway (C1q binding) by mesophilic *Aeromonas hydrophila* outer membrane protein. *Infect. Immun.* **66**:3825–3831.
- Merino, S., X. Rubires, S. Knochel, and J. M. Tomas. 1995. Emerging pathogens: *Aeromonas* spp. *Int. J. Food Microbiol.* **28**:157–168.
- Merino, S., X. Rubires, A. Aguilar, S. Alberti, S. Hernandez-Alles, V. J. Benedi, and J. M. Tomas. 1996. Mesophilic *Aeromonas* sp. serogroup O:11 resistance to complement-mediated killing. *Infect. Immun.* **64**:5302–5309.
- Mulin, J. M., and K. V. Snock. 1990. Effect of tumor necrosis factor on epithelial tight junctions and transepithelial permeability. *Cancer Res.* **50**:2172–2176.
- Parker, M. W., F. G. van der Goot, and J. T. Buckley. 1996. Aerolysin—the ins and outs of a channel forming protein. *Mol. Microbiol.* **19**:205–212.
- Peitsch, M. C., C. Borner, and J. Tschopp. 1993. Sequence similarity of phospholipase A₂-activating protein and the G β -subunits: a new concept of

- effector protein activation in signal transduction. *Trends Biochem. Sci.* **18**: 292–293.
52. Pemberton, J. M., S. P. Kidd, and R. Schmidt. 1997. Secreted enzymes of *Aeromonas*. *FEMS Microbiol. Lett.* **152**:1–10.
 53. Peterson, J. W., and L. Ochoa. 1989. Role of prostaglandins and cAMP in the secretory effects of cholera toxin. *Science* **245**:857–859.
 54. Peterson, J. W., S. S. Saini, W. D. Dickey, G. R. Klimpel, J. S. Bomalaski, M. A. Clark, X. J. Xu, and A. K. Chopra. 1996. Cholera toxin induces synthesis of phospholipase A₂-activating protein. *Infect. Immun.* **64**:2137–2143.
 55. Potomski, J., V. Burke, J. Robinson, D. Fumarola, and G. Miragliotta. 1987. *Aeromonas* cytotoxic enterotoxin cross-reactive with cholera toxin. *J. Med. Microbiol.* **13**:179–186.
 56. Potomski, J., V. Burke, I. Watson, and M. Gracey. 1987. Purification of cytotoxic enterotoxin of *Aeromonas sobria* by use of monoclonal antibodies. *J. Med. Microbiol.* **23**:171–177.
 57. Pugazhenth, S., E. Miller, C. Sable, P. Young, K. A. Heidenreich, L. M. Boxer, and J. E. B. Reusch. 1999. Insulin-like growth factor-1 induces *bcl-2* promoter through the transcription factor cAMP-response element binding protein. *J. Biol. Chem.* **274**:27529–27535.
 58. Rose, J. M., C. W. Houston, D. H. Coppenhaver, J. D. Dixon, and A. Kurosky. 1989. Purification and chemical characterization of a cholera toxin-cross-reactive cytolytic enterotoxin produced by a human isolate of *Aeromonas hydrophila*. *Infect. Immun.* **57**:1165–1169.
 59. Rose, J. M., C. W. Houston, and A. Kurosky. 1989. Bioactivity and immunological characterization of a cholera toxin-cross-reactive cytolytic enterotoxin from *Aeromonas hydrophila*. *Infect. Immun.* **57**:1170–1176.
 60. Rossjohn, J., R. J. Gilbert, D. Crane, P. J. Morgan, T. J. Mitchell, A. J. Rowe, P. W. Andrew, J. C. Paton, R. K. Tweten, and M. W. Parker. 1998. The molecular mechanism of pneumolysin, a virulence factor from *Streptococcus pneumoniae*. *J. Mol. Biol.* **284**:449–461.
 61. Saini, S. S., A. K. Chopra, and J. W. Peterson. 1999. Melittin activates endogenous phospholipase D during cytolysis of human monocytic leukemia cells. *Toxicon* **37**:1605–1619.
 62. Saini, S. S., J. W. Peterson, and A. K. Chopra. 1997. Melittin binds to secretory phospholipase A₂ and inhibits its enzymatic activity. *Biophys. Biochem. Res. Commun.* **238**:436–442.
 63. Shenkar, R., and E. Abraham. 1999. Mechanisms of lung neutrophil activation after hemorrhage or endotoxemia: roles of reactive oxygen intermediates, NF- κ B, and cyclic AMP response element binding protein. *J. Immunol.* **163**:954–962.
 64. Taylor, C. T., N. Fueki, A. Agah, R. M. Hershberg, and S. P. Colgan. 1999. Critical role of cAMP response element binding protein expression in hypoxia-elicited induction of epithelial tumor necrosis factor- α . *J. Biol. Chem.* **274**:19447–19454.
 65. Tesh, V. L., B. Ramegowda, and J. E. Samuel. 1994. Purified Shiga-like toxins induce expression of proinflammatory cytokines from murine peritoneal macrophages. *Infect. Immun.* **62**:5085–5094.
 66. Wadstrom, T., A. Ljungh, and B. Wretling. 1976. Enterotoxin, haemolysin and cytotoxic protein in *Aeromonas hydrophila* from human infections. *Acta Pathol. Microbiol. Scand. Sect. B* **84**:112–114.
 67. Wang, Z., and H. H. Tai. 1999. Cyclic AMP response element mediates dexamethasone induced suppression of prostaglandin H synthase-2 gene expression in human amnion derived WISH cells. *Prostaglandins Leuko. Essent. Fatty Acids* **60**:243–248.
 68. Xie, Q. W., Y. Kashiwabara, and C. Nathan. 1994. Role of transcription factor NF- κ B/Rel in induction of nitric oxide synthase. *J. Biol. Chem.* **269**:4705–4708.
 69. Xu, X. J., M. R. Ferguson, V. L. Popov, C. W. Houston, J. W. Peterson, and A. K. Chopra. 1998. Role of a cytotoxic enterotoxin in *Aeromonas*-mediated infections: development of transposon and isogenic mutants. *Infect. Immun.* **66**:3501–3509.
 70. Yamada, S., S. Matsushita, S. Dejsirilet, and Y. Kudoh. 1997. Incidence and clinical symptoms of *Aeromonas*-associated travellers' diarrhoea in Tokyo. *Epidemiol. Infect.* **119**:121–126.
 71. Zhang, Y., J. Lemasters, and B. Herman. 1999. Secretory group IIA phospholipase A₂ generates anti-apoptotic survival signals in kidney fibroblasts. *J. Biol. Chem.* **274**:27726–27733.

Editor: J. D. Clements